Mat. Res. Bull., Vol. 19, pp. 83-92, 1984. Printed in the USA.
0025-5408/84 $3.00 + .00

THE LUMINESCENCE OF BISMUTH AND MANGANESE IN $LaMgB_5O_{10}$

Michel Saakes, Markku Leskelä * and George Blasse,
Physical Laboratory, State University, P.O. Box 80.000
3508 TA Utrecht, The Netherlands

(Received September 22, 1983; Communicated by W. B. White)

ABSTRACT

The luminescences of Bi^{3+} and Mn^{2+} in $LaMgB_5O_{10}$ are reported. The emission of the Bi^{3+} ion shows a small Stokes shift and is situated in the ultraviolet. From the decay times the $^3P_0$ and $^3P_1$ levels appear to be mixed. At 4.2 K no energy transfer between Bi^{3+} ions occurs, but at room temperature the critical distance for this energy transfer amounts to some 25 Å. This knowledge is used to explain energy transfer between Bi^{3+} and Tb^{3+} in $LaMgB_5O_{10}$, which is compared with that between Ce^{3+} and Tb^{3+} in the same lattice. The Mn^{2+} ion shows a red emission in $LaMgB_5O_{10}$. The Bi^{3+} ion acts as a sensitizer for this emission, whereas the Ce^{3+} ion does not.

Introduction

The crystal structure of $LaMgB_5O_{10}$ has been reported recently (1) and is isomorphous with that of $SmCoB_5O_{10}$ (2). The La^{3+} ion can be replaced by the smaller rare earth ions up to Er^{3+} without change of crystal structure (1). The La^{3+} ions are in an irregular ten-coordination and their crystallographic site does not contain symmetry elements. The Mg^{2+} ions occupy a distorted octahedral site. The La^{3+} ions form a linear zig-zag chain in which the La^{3+} - La^{3+} distance is about 4.0 Å; the shortest distance between La^{3+} ions in different chains is about 6.4 Å. The La^{3+} sublattice has a one-dimensional character, therefore.

Several rare earth ions have been shown to luminesce efficiently in this lattice, e.g. Ce^{3+}, Eu^{3+} and Tb^{3+} (3,4). In this paper we wish to report the luminescence of some non-rare-earth ions in this host lattice, viz. Bi^{3+}

* On leave of absence from Dept. of Chemistry, University of Oulu, Finland.

on La^{3+} sites and Mn^{2+} on Mg^{2+} sites. Both show luminescence with high efficiency in $LaMgB_5O_{10}$. In addition we studied a number of energy transfer phenomena, viz. Bi^{3+} - Bi^{3+}, Bi^{3+} - Tb^{3+}, Ce^{3+} - Tb^{3+} and the sensitisation of the Mn^{2+} luminescence. A preliminary report was published recently (5). In a subsequent paper we will report on the luminescence of activators in $GdMgB_5O_{10}$ where the one-dimensional character of the Gd^{3+} sublattice is of importance.

Experimental

All samples were prepared as described in the literature (1,3,4). Starting materials were dissolved in nitric acid with an excess of boric acid. The solutions were evaporated till dryness. Firing was performed in air or in a slightly reducing atmosphere depending on the nature of the activator. Under flowing atmosphere an excess of 100% and under static atmosphere an excess of 10% boric acid was used. Samples were checked by X-ray powder diffraction. Possible impurities were found to be LaB_3O_6 and MgB_2O_5.

Optical measurements were performed as described before (6). The spectrometer is a Perkin-Elmer MPF-3 spectrofluorometer. The sample was cooled to liquid helium temperature in an Oxford CF 100 flow cryostat. Decaytime measurements were performed with a single-photon-counting setup described recently (7).

Results

Samples of $La_{1-x}Bi_xMgB_5O_{10}$ ($x < 0.02$) show an efficient ultraviolet emission at liquid helium temperature (LHeT) and room temperature (RT). By comparison with standard phosphors the quantum efficiency is found to be 70% or higher. Fig. 1 shows the relevant emission and excitation spectra of this luminescence.

It was possible to replace up to 30% of the La^{3+} ions by Bi^{3+} ions. For higher amounts of Bi^{3+} no single-phase formation was observed. The quantum efficiency of the Bi^{3+} emission appears to be independent of x at LHeT. At RT, however, concentration quenching was observed above a critical Bi^{3+} concentration of about 2% ($x_c \approx 0.02$). Fig. 2 presents the intensity of the Bi^{3+} luminescence of $La_{1-x}Bi_xMgB_5O_{10}$ as a function of x at RT.

Diffuse reflection spectra of $LaMgB_5O_{10}$: Bi at RT show broad absorption bands at about 300 and 250 nm. The former corresponds clearly to the excitation maximum at about 300 nm (fig. 1). No clear excitation band was observed at higher energies (i.e. corresponding to the latter absorption band). This is probably due to the poor performance of the spectrofluorometer in this spectral region (it is equipped with a xenon lamp). Note that the emission maximum of the Bi^{3+} luminescence shifts to higher energies with increasing temperature (345 nm at LHeT to 335 nm at RT). From these values we derive a Stokes shift of about 4500 cm^{-1} at LHeT which is a rather small value.

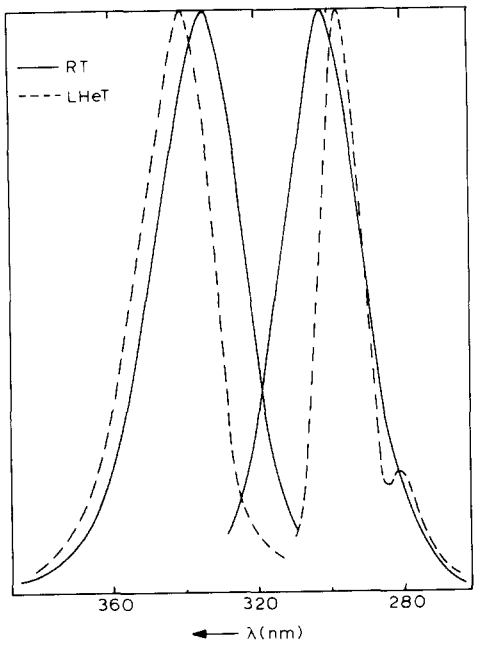

FIG. 1

Emission and excitation spectra of the luminescence of $La_{0.99}Bi_{0.01}MgB_5O_{10}$ at RT and LHeT. Uncorrected recorder curves. Corrections would raise the shorter wavelength side of the excitation spectra.

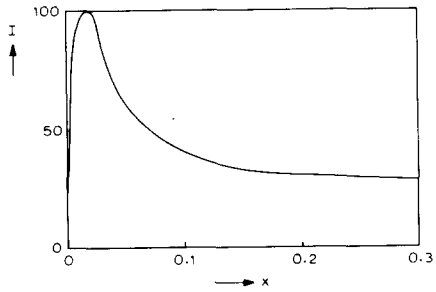

FIG. 2

The intensity of the Bi^{3+} luminescence of $La_{1-x}Bi_xMgB_5O_{10}$ at room temperature as a function of x. Excitation is into the $^1S_0 \rightarrow {}^3P_1$ transition of the Bi^{3+} ion.

In addition we prepared $Y_{0.97}Bi_{0.03}MgB_5O_{10}$. The yttrium composition has also the crystal structure of $LaMgB_5O_{10}$, as is to be expected in view of the results for smaller rare earth ions mentioned above. Although the luminescence spectra of $YMgB_5O_{10}$: Bi are similar to those of $LaMgB_5O_{10}$: Bi, there are some clear differences. The maximum of the excitation band has shifted from 300 nm for the La compound to 270 nm for the Y case. The emission of the Y sample is only 10 nm shifted to shorter wavelength in comparison with that of the La sample. This means that the Stokes shift for $YMgB_5O_{10}$: Bi is larger than for $LaMgB_5O_{10}$: Bi. It amounts to about 7000 cm^{-1}. Consequently, the spectra of the Y sample were considerably broader: for the emission band at LHeT the half width is 40 nm for the Y sample and 25 nm for the La sample. The Y sample was not investigated further.

Decaytime measurements were performed on La samples with low bismuth concentrations. The decay curves were slightly curved for short times after the pulse for x = 0.03 and considerably less so for x = 0.003. Further they were singly exponential. Decay times were derived from the exponential part of the curve and are given in fig. 3 as a function of temperature. Since the luminescence efficiency is temperature independent up till RT, the temperature dependence of the decay time points to a three (or even more) level scheme. A reasonable fit was obtained with a three-level scheme (fig. 4) with $\Delta E = 430\ cm^{-1}$, $p_{10}^{-1} = 13\ \mu s$ and $p_{20}^{-1} = 0.2\ \mu s$ assuming thermal equilibrium between the levels 1 and 2. The p^{-1} values are relatively exceptional for Bi^{3+} in oxides and will be discussed below.

A sample of $LaMg_{0.97}Mn_{0.03}B_5O_{10}$ shows a weak deep-red emission under

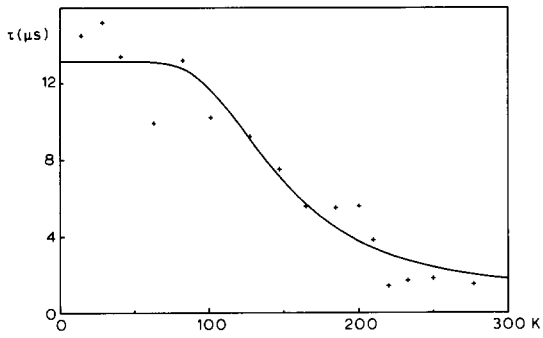

FIG. 3

Decay times of the Bi^{3+} luminescence of $La_{0.99}Bi_{0.01}MgB_5O_{10}$ as a function of temperature.

ultraviolet excitation. The intensity is temperature independent up till RT. The emission spectrum consists of a band with a halfwidth of about 70 nm and a maximum at about 620 nm (see fig. 5). Its emission spectrum contains the well-known crystal-field transitions for a d^5 ion (8). Fig. 5 shows only those in the uv spectral region. These are of relevance for the discussion below.

By comparison with red-emitting standard phosphors the quantum efficiency of the Mn^{2+} emission was estimated to be (80±20)% at RT and LHeT. Due to the low absorption strength of the Mn^{2+} ion, this value is not very accurate. The low luminescence intensity is, therefore, due to weak absorption and not to a low conversion efficiency. Since Mn^{2+} occupies an octhahedral site, the excitation transitions are spin- and parity-forbidden. The host lattice absorption is situated below 200 nm (4), which is outside the spectral range of our spectrofluorometer. Under ion bombardment, however, a red emission of reasonable intensity was observed, so that transfer from the host lattice to the Mn^{2+} ion occurs.

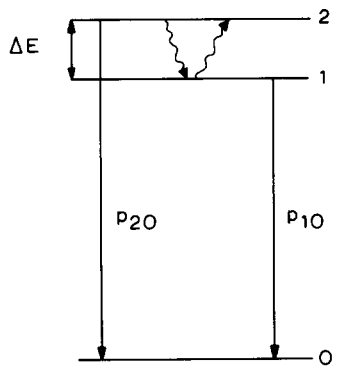

FIG. 4

Three-level scheme for the Bi^{3+} ion. Radiative transition probabilities are given by p.

In order to sensitize the Mn^{2+} emission we prepared codoped samples $LaMgB_5O_{10}$: M,Mn (M = Ce or Bi). In the case of Ce^{3+} no sensitisation of any importance was observed: excitation into the Ce^{3+} absorption bands (4) resulted in mainly Ce^{3+} emission and practically no Mn^{2+} emission. The Bi^{3+} ion is more successful this aspect: for a sample with composition $La_{0.97}Bi_{0.03}Mg_{0.95}Mn_{0.05}B_5O_{10}$, for example, we found at RT a Mn^{2+}/ Bi^{3+} emission-intensity ratio of about 1.0 upon Bi^{3+} excitation. At LHeT the transfer efficiency decreases considerably, viz. about one order of magnitude.

These results prompted us to investigate also codoped samples with another activator. For this reason we prepared samples $LaMgB_5O_{10}$: M,Tb^{3+} (M = Bi^{3+} or Ce^{3+}). In fig. 6 we have plotted the amount of Tb^{3+} emission for a series of compositions $La_{0.97-x}Tb_xBi_{0.03}MgB_5O_{10}$ for excitation into the Bi^{3+} ion. The amount of Tb^{3+} emission increases rapidly with the Tb^{3+} concentration (x). This increase is more rapid for LHeT than for RT, so that the overall transfer efficiency for $Bi^{3+} \rightarrow Tb^{3+}$ transfer decreases with increasing temperature. The results of fig. 6 are typical for Bi^{3+}, Tb^{3+} codoped samples, so that other compositions

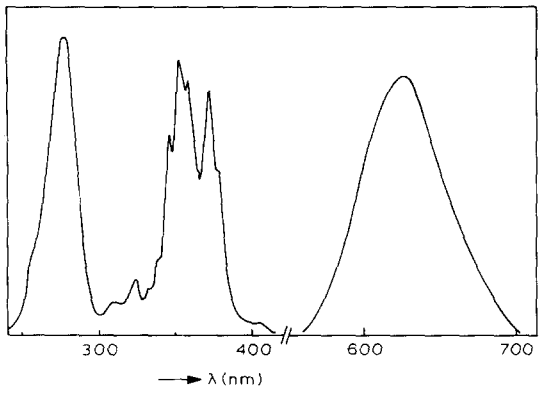

FIG. 5

Emission and excitation spectra of the Mn^{2+} emission of $LaMg_{0.97}Mn_{0.03}B_5O_{10}$ at RT. Note change in wavelength scale. Uncorrected recorder curves. Corrections would raise the shortest wavelength excitation band.

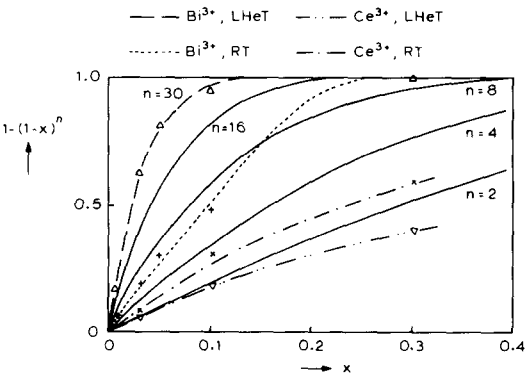

FIG. 6

The function $1-(1-x)^n$ as a function of x for several values of n (see text). The amount of Tb^{3+} emission in the total emission of $La_{0.97-x}Bi_{0.03}Tb_xMgB_5O_{10}$ and of $La_{0.9-x}Ce_{0.1}Tb_xMgB_5O_{10}$ upon Bi^{3+} or Ce^{3+} excitation is given as a function of x for RT and LHeT. Symbols indicate experimental points.

will not be discussed. However, these results are different from those reported by Saubat et al. (4) for Ce^{3+}, Tb^{3+} codoped samples. These authors find a less rapid increase of the amount of Tb^{3+} emission with increasing Tb^{3+} concentration than given for Bi^{3+} in fig. 6. We repeated their work and extended it to LHeT for the series $La_{0.9-x}Tb_xCe_{0.1}MgB_5O_{10}$. Results are also given in fig. 6 and are in good agreement with ref. 4. Note the much slower increase of the curves in comparison with the ones for Bi^{3+} - Tb^{3+} codoped samples and the small difference between the RT and LHeT values for the Ce^{3+} - Tb^{3+} codoped samples.

Discussion

a. The Bi^{3+} emission

The Bi^{3+} ion has $6s^2$ ground state configuration. Its luminescence properties are usually discussed in an energy level scheme $^1S_0 < ^3P_0 < ^3P_1 < ^3P_2 < ^1P_1$ (9). In this way a straightforward assignment of the spectra follows. The bands in the reflection spectra are the only allowed transitions, viz. $^1S_0 \rightarrow ^3P_1$ (300 nm) and $^1S_0 \rightarrow ^1P_1$ (250 nm). The excitation band is, therefore, also assigned to $^1S_0 \rightarrow ^3P_1$. The emission transition at low temperatures is the $^3P_0 \rightarrow ^1S_0$ transition. At higher temperatures, however, the emission is mainly $^3P_1 \rightarrow ^1S_0$ due to thermal equilibrium between the $^3P_0$ and $^3P_1$ levels and the higher transition probability of the $^3P_1 \rightarrow ^1S_0$ transition (10).

This assignment is confirmed by the results of the decay time measurements. Usually, however, the $^3P_0 \rightarrow {}^1S_0$ transition probability is about one order of magnitude smaller and the $^3P_1 \rightarrow {}^1S_0$ transition probability about one order of magnitude larger (10). This observation is ascribed to the absence of any symmetry elements, even approximate symmetry elements, on the crystallographic site occupied by the Bi^{3+} ion. In the C_1 group the $^3P_1$ level splits into three levels which have the same representation as the $^3P_0$ level. This means that the $^3P_0$ level and the $^3P_1$ levels may mix, which is usually only possible by higher-order perturbations. The mixing of the $^3P_0$ and $^3P_1$ levels is reflected in the exceptional values of the transition probabilities.

A relation between the Stokes shift and the energy difference between the $^3P_0$ and $^3P_1$ level has been given earlier (11). In view of the present Stokes shift we expect a larger $\Delta(^3P_1-{}^3P_0)$ than the 430 cm^{-1} found from the decay times. However, a crystal-field splitting of the $^3P_1$ level, as is to be expected under the present low site-symmetry, will depress the value of Δ. Further it should be realized, that the LS coupling scheme will certainly have its limitations for the Bi^{3+} ion, as argued and examplified elsewhere (7).

For Bi^{3+} in $YMgB_5O_{10}$ the assignment of the transitions can be similar. Usually the value of the Stokes shift decreases if the host lattice ion becomes smaller (12,13). The present case seems to be exceptional, but the same observation has been made for the oxychlorides LnOCl : Bi (14). Evidence was presented that the Bi^{3+} ions in YOCl occur in pairs, so that comparison with the isolated Bi^{3+} ions in LaOCl is not justified. It remains to be investigated whether the Bi^{3+} ions in $YMgB_5O_{10}$ occur also in pairs. In this connection it may be remarked that the nonexponential part in the decay curves of the emission of $LaMgB_5O_{10}$: Bi can be due to emission from Bi^{3+} pairs, since it is only observed for higher concentrations. These effects will be studied in the future.

The Stokes shift of Bi^{3+} in $LaMgB_5O_{10}$ is relatively small (11). It is well known that a small Stokes shift leads to high thermal quenching temperatures of the emission and to low critical concentrations for concentration quenching (15). This was observed also for the Bi^{3+} luminescence in $LaMgB_5O_{10}$ at RT. From $x_c = 0.02$ and the crystallographic data it is possible to calculate the critical distance for energy transfer (R_c) between two Bi^{3+} ions in $LaMgB_5O_{10}$ at RT (16). This yields a value of about 25 Å for R_c, a rather long distance. By using the spectral data at RT for a sample $La_{0.997}Bi_{0.003}MgB_5O_{10}$ and the oscillator strength of the $^1S_0 - {}^3P_1$ transition, it is possible to arrive at a value of R_c in a completely different way (16). This value amounts also 25 Å. The agreement between both values is certainly flattered in view of the inaccuracies involved. It shows, nevertheless, that energy transfer between Bi^{3+} ions in $LaMgB_5O_{10}$ at RT can proceed over at least 20 Å.

At LHeT, however, no concentration quenching occurs up till 30% Bi^{3+}. This suggests strongly the vanishing of energy transfer between Bi^{3+} ions at LHeT. In fact the spectral overlap of the emission and excitation bands vanishes at LHeT (see fig. 1). Since emission and excitation correspond to different transitions at LHeT, the vanishing of the spectral overlap is no argument against energy migration. Kellendonk et al. (17) have shown that in

$YAl_3B_4O_{12}$: Bi energy transfer between Bi^{3+} ions occurs, even at LHeT and in spite of a vanishing spectral overlap. This is possible, because in $YAl_3B_4O_{12}$ the energy transfer occurs via the $^3P_1$ levels, i.e. the transfer rate via the $^3P_1$ levels exceeds the rate of nonradiative decay to the $^3P_0$ level. In the case of $YAl_3B_4O_{12}$: Bi these rates were estimated to be 3×10^{10} s^{-1} and $\sim 10^9$ s^{-1} (17), respectively. The $^3P_1$ - $^3P_0$ nonradiative rate is expected to be faster for Bi^{3+} in $LaMgB_5O_{10}$ than for Bi^{3+} in $YAl_3B_4O_{12}$, because the relevant energy gaps are 430 and 1100 cm^{-1}, respectively. The higher the energy gap, the lower the nonradiative rate. The $Bi^{3+} \rightarrow Bi^{3+}$ transfer rate, P_{Bi-Bi}, is expected to be lower for Bi^{3+} in $LaMgB_5O_{10}$ than for Bi^{3+} in $YAl_3B_4O_{10}$. The reason for this is the smaller spectral overlap (no vibrational structure observed) and the lower $^1S_0 \rightarrow {}^3P_1$ transition probability (see above). Since $P_{Bi-Bi} \sim Q^2_{Bi}.R^6_{Bi-Bi}.SO$, where SO denotes the spectral overlap and Q the absorption strength, and Q_{Bi} is an order of magnitude smaller in $LaMgB_5O_{10}$, P_{Bi-Bi} will be smaller in $LaMgB_5O_{10}$. This is true, even after correction for distance (R_{Bi-Bi} is 6 Å in $YAl_3B_4O_{12}$ and 4 Å in $LaMgB_5O_{10}$).

If for Bi^{3+} in $LaMgB_5O_{10}$, the $^3P_1 \rightarrow {}^3P_0$ nonradiative rate exceeds the transfer rate at LHeT, energy transfer between Bi^{3+} ions becomes impossible, the transfer rate via the $^3P_0$ levels being negligible (17). Our estimates given above confirm such a model. This presents an interesting difference between Bi^{3+} in $YAl_3B_4O_{12}$ and Bi^{3+} in $LaMgB_5O_{10}$ at LHeT. In the former excitation into the $^3P_1$ level may be followed by transfer to other Bi^{3+} ions, because this is a more probable process than nonradiative decay to $^3P_0$. In $LaMgB_5O_{10}$, however, transfer is impossible, because the nonradiative decay to $^3P_0$ is the more probable process. At room temperature this difference does not longer exist, because the $^3P_1$ level is then thermally populated. We conclude that our estimates of the rates of the several processes involved confirm the conclusion from the absence of concentration quenching of the Bi^{3+} luminescence in $LaMgB_5O_{10}$ at LHeT, viz. that no energy transfer between Bi^{3+} ions occurs.

b. The Mn^{2+} emission

The emission and excitation bands of the Mn^{2+} luminescence of $LaMgB_5O_{10}$: Mn are those which are to be expected for octahedrally coordinated Mn^{2+}. The emission transition is $^4T_1 \rightarrow {}^6A_1$, for example. We used Ce^{3+} and Bi^{3+} to sensitize the Mn^{2+} emission. The Ce^{3+} ion, however, does not transfer its excitation energy to the Mn^{2+} ion. The reason for this is obvious. The Ce^{3+} emission band peaks at about 310 nm (4). It shows, therefore, a very poor spectral overlap with the Mn^{2+} excitation bands (see fig. 5). The Bi^{3+} emission is more favourable in this aspect (compare figs. 1 and 5). At LHeT the efficiency of $Bi^{3+} \rightarrow Mn^{2+}$ energy transfer is still poor. The oscillator strength of the Mn^{2+} ion at LHeT is very low, since the transition involved is vibronically assisted (8). Also the Mn^{2+} absorption lines involved sharpen at LHeT, so that the spectral overlap may be low. Unfortunately we were not able to measure this accurately. It is therefore impossible to speculate on the transfer mechanism.

At RT the oscillator strength and the spectral overlap are larger. They

appear to be high enough to allow $Bi^{3+} \rightarrow Mn^{2+}$ energy transfer. Since $Sb^{3+} \rightarrow Mn^{2+}$ transfer has been shown to occur by exchange (18), the same may be true for the $Bi^{3+} \rightarrow Mn^{2+}$ transfer. Above it was shown that $Bi^{3+} \rightarrow Bi^{3+}$ energy transfer can cover large distances, so that the situation at RT in samples of $LaMgB_5O_{10} : Bi^{3+}, Mn^{2+}$ is probably very complicated. We decided to investigate this, using an activator which allows also energy transfer at LHeT. The Tb^{3+} ion appeared to be favourable in this aspect.

c. Energy transfer from Bi^{3+} to Tb^{3+}.

The Tb^{3+} luminescence in $LaMgB_5O_{10}$ has been described in refs. 3 and 4. Characteristic results for the system $(La,Bi,Tb)MgB_5O_{10}$ are presented in fig. 6. Our LHeT results are discussed first, because they should be relatively simple. This is due to the fact that $Bi^{3+} \rightarrow Bi^{3+}$ energy transfer does not occur at LHeT (see above). It is only necessary to compare the probability for Bi^{3+} radiative emission and the $Bi^{3+} \rightarrow Tb^{3+}$ transfer probability, assuming that excitation is in the Bi^{3+} ion.

If the Tb^{3+} concentration is denoted by x, the probability to find no Tb^{3+} on a La^{3+} site in $(La,Bi,Tb)MgB_5O_{10}$ is 1-x. Let n be the number of La^{3+} sites within a sphere with radius R_c around a Bi^{3+} ion, where R_c is the critical distance for $Bi^{3+} \rightarrow Tb^{3+}$ energy transfer. If none of these sites is occupied by Tb^{3+}, the central Bi^{3+} ion will emit Bi^{3+} luminescence upon excitation. If one (or more) of the n sites is occupied by Tb^{3+}, Tb^{3+} emission will appear after Bi^{3+} excitation. The probability that the n sites are not occupied by Tb^{3+} is $(1-x)^n$. The probability for Tb^{3+} emission is, therefore, $1-(1-x)^n$. This function is plotted in fig. 6 for several values of n. The LHeT values fit to n = 30. With the crystallographic data this yields for R_c at LHeT about 11 Å.

It is possible to calculate R_c from the spectral data obtained and the oscillator strength values given in the literature (19). This yields only 8 Å. The discrepancy between these two values cannot be accounted for by an inaccuracy in the measurements. We, therefore, assume that the $Bi^{3+} \rightarrow Bi^{3+}$ transfer efficiency does not vanish completely, i.e. the $Bi^{3+} - Bi^{3+}$ transfer rate via the $^3P_1$ levels is not very much smaller than the nonradiative $^3P_1 \rightarrow {}^3P_0$ transition rate. In this way transfer between near Bi^{3+} ions may be possible. If on the average the Bi^{3+} excitation energy migrates a few Å, the difference between the R_c values is explained, without violating the argument given above in connection with the absence of concentration quenching of Bi^{3+} luminescence at LHeT.

Fig. 6 shows that the RT values do not obey the relation $1-(1-x)^n$. At room temperature the R_c value calculated from spectral data is somewhat smaller than at LHeT, viz. 6.5 Å. This is due to a smaller spectral overlap. This distance covers only the nearest and next-nearest neighbours, the number of which is about 8. However, we have to add to this 6.5 Å at least a few Å in view of $Bi^{3+} \rightarrow Bi^{3+}$ transfer which at room temperature will be certainly more effective than at LHeT. Since our experimental curve falls only in the neighbourhood of the n = 8 curve, we have to conclude that there is a discrepancy between the model used successfully at LHeT and the RT experimental

results. This shows the influence of efficient $Bi^{3+} \rightarrow Bi^{3+}$ energy transfer which suppresses the total Tb^{3+} output. This is because the excitation energy will tend to remain in a system of mutually transferring Bi^{3+} ions. Although their concentration will be low for 3% Bi, this effect will decrease the Tb^{3+} output calculated according to $1-(1-x)^n$. In principle this is a 'microcase' of fast diffusion: from the estimates given above it is clear that at RT the $Bi^{3+} \rightarrow Bi^{3+}$ transfer rate exceeds the $Bi^{3+} \rightarrow Tb^{3+}$ transfer rate strongly for the same distances. For the high Tb^{3+} concentration this effect will be less outspoken. The Tb^{3+} ions are now, due to their high concentration, able to accept the transferred excitation energy. We have refrained from further analysis, which seems to be difficult. Further the experimental inaccuracy is not negligible. Nevertheless the present model gives a rather accurate idea about the transfer processes which play a role. The more efficient total transfer rate at LHeT is due to a higher $Bi^{3+} - Tb^{3+}$ transfer rate and a lower $Bi^{3+} - Bi^{3+}$ transfer rate at LHeT. Let us now compare these results with those reported in the literature for the system $(La,Ce,Tb)MgB_5O_{10}$ (4).

d. Energy transfer from Ce^{3+} to Tb^{3+}

Fig. 6 shows that our LHeT results for the system $La_{0.9-x}Ce_{0.1}Tb_xB_5O_{10}$ are close to the function $1-(1-x)^n$ for n = 2. This suggests that at LHeT $Ce^{3+} \rightarrow Ce^{3+}$ transfer is negligible and $Ce^{3+} \rightarrow Tb^{3+}$ transfer is restricted to nearest neighbours in the chain. From the spectral data we calculated R_c for $Ce^{3+} \rightarrow Tb^{3+}$ transfer as indicated in ref. 16. We find 5.5 Å for LHeT and RT. Since the shortest interchain distance is about 6.4 Å, this shows that the $Ce^{3+} \rightarrow Tb^{3+}$ transfer is restricted to the chains. Our spectra did not reveal vibrational structure in the Ce^{3+} spectra at LHeT, so that the $Ce^{3+} \rightarrow Ce^{3+}$ transfer probability vanishes at low temperatures (20).

The values at RT are somewhat higher than the n = 2 curve (see fig. 6). The R_c value for $Ce^{3+} \rightarrow Ce^{3+}$ transfer at RT was estimated from the critical Ce^{3+} concentration (4) and the spectral data. Both methods yield about 14 Å. This suggests that some $Ce^{3+} \rightarrow Ce^{3+}$ transfer occurs in our experiments, where the Ce^{3+} concentration was 10%, i.e. equal to the critical concentration. Our data show that its influence on the total $Ce^{3+} \rightarrow Tb^{3+}$ transfer efficiency is not very large for the 10% Ce^{3+} concentration. Saubat et al. (4) have also studied samples with higher concentration of Ce^{3+}. Their results show the importance of $Ce^{3+} - Ce^{3+}$ transfer. There is no doubt, however, that the total $Bi^{3+} \rightarrow Tb^{3+}$ transfer efficiency exceeds that of the total $Ce^{3+} \rightarrow Tb^{3+}$ transfer, since R_c at RT is larger for $Bi^{3+} \rightarrow Bi^{3+}$ than for $Ce^{3+} \rightarrow Ce^{3+}$ transfer and also larger for $Bi^{3+} \rightarrow Tb^{3+}$ than for $Ce^{3+} \rightarrow Tb^{3+}$ transfer. We will show elsewhere that the total $Ce^{3+} \rightarrow Tb^{3+}$ transfer efficiency can be increased enormously by using the Gd^{3+} sublattice, whereas the Bi^{3+}, Tb^{3+} system does not profit from this (21).

Acknowledgements

One of the authors (M.L.) acknowledges gratefully financial aid from the Academy of Finland.

References

1. B. Saubat, M. Vlasse and C. Fouassier, J. Solid State Chem. 34, 271 (1980).
2. G.K. Abdullaev, K.S. Mamedov and G.G. Dzhafarov, Sov. Phys. Crystallogr. 19, 457 (1975).
3. C. Fouassier, B. Saubat and P. Hagenmuller, J. Luminescence 23, 405 (1981).
4. B. Saubat, C. Fouassier and P. Hagenmuller, Mater. Res. Bull. 16, 193 (1981).
5. M. Saakes and G. Blasse, Phys. Stat. Sol. (a) 78, K97 (1983).
6. H. Ronde and G. Blasse, J. Inorg. Nucl. Chem. 40, 215 (1978).
7. C.W.M. Timmermans and G. Blasse, J. Solid State Chem., to be published.
8. See e.g. C.J. Ballhausen, Introduction to Ligand Field Theory, McGraw-Hill, New York, 1962.
9. G. Blasse and A. Bril, J. Chem. Phys. 48, 217 (1968).
10. See e.g. G. Boulon, J. Physique 36, 267 (1975).
11. G. Blasse and A.C. van der Steen, Solid State Comm. 31, 993 (1979).
12. A.C. van der Steen, J.J.A. van Hesteren and A.P. Slok, J. Electrochem. Soc. 128, 1327 (1981).
13. A. Wolfert, M. Oomen, G. Blasse, to be published.
14. A. Wolfert and G. Blasse, Mater. Res. Bull., in press.
15. G. Blasse, in Luminescence of Inorganic Solids (Ed. B. DiBartolo), Plenum Press, New York, 1978, page 457 sq.
16. G. Blasse, Philips Res. Repts. 24, 131 (1969).
17. F. Kellendonk, T. van den Belt and G. Blasse, J. Chem. Phys. 76, 1194 (1982).
18. T.F. Soules, R.L. Bateman, R.A. Hewes and E.R. Kreidler, Phys. Rev. B, 7, 1657 (1973).
19. W.T. Carnall, Chapter 24 in Handbook on the Physics and Chemistry of Rare Earths, Vol. 3 (eds. K.A. Gschneider Jr, LeRoy Eyring), North Holland, Amsterdam 1979.
20. R.C. Powell and G. Blasse, Structure and Bonding, 42, 43 (1980).
21. M. Leskelä, M. Saakes and G. Blasse, Mater. Res. Bull., to be published; see also J.Th.W. de Hair and J.T.C. van Kemenade, paper no 54 3rd Int. Conf. Science and Technology of Light Sources, Toulouse, 1983.